Electronic supplementary information (ESI)

Cumulative Gain in Organic Solar Cells by Using Multiple Optical Nanopatterns

*Soo Won Heo, Le Hac Huong Thu, Takuo Tanaka, Itaru Osaka, Kazuo Takimiya and Keisuke Tajima**

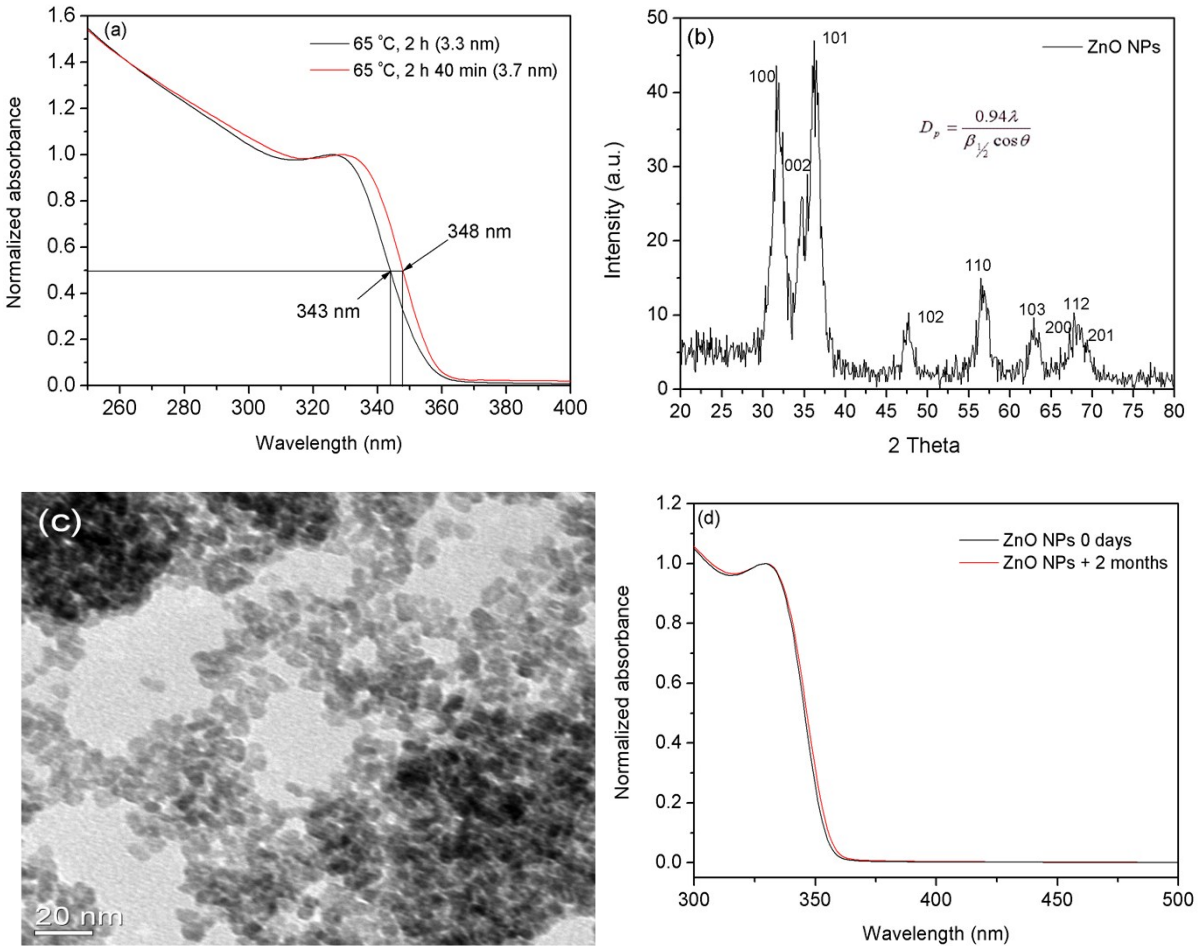

Fig. S1 Characterization of ZnO NPs. (a) UV-vis absorption spectra of ZnO NPs in chloroform solution synthesized with different reaction times, (b) powder X-ray diffraction pattern, and (c) FE-TEM image. (d) UV-vis absorption spectra of ZnO NPs in chloroform solution after 2 month storage to show the stability of ZnO NPs.

Characterization of ZnO nanoparticles

Fig. S1a shows the UV absorbance of synthesized ZnO nanoparticles with different synthesis conditions. As the reaction time increased, a slight red shift in the absorption spectra of the NPs was observed, indicating a marginal increase in the size of the ZnO NPs. The ZnO NP size was calculated from the absorption wavelength by using the empirical formula[1]

$$\frac{1240}{\lambda_{1/2}} = 3.301 + \frac{294}{D^2} + \frac{1.09}{D} \qquad (1)$$

where $\lambda_{1/2}$ is the wavelength at which the absorption is 50% that at the shoulder peak, and D is the diameter of ZnO in Angstroms. This equation gave a good description of the experimental size dependence for 25 Å < D < 65 Å and was used to convert experimental values of $\lambda_{1/2}$ into particle size. Following this equation, the ZnO NP diameters were calculated to be about 3.7 nm. Fig. S1b shows the XRD diffraction patterns of ZnO NPs. The average crystallite size was ~4.1 nm, estimated by the Scherrer equation (inset) for the (100), (002), and (101) diffraction peaks. Fig. S1c shows the transmission electron microscopy (TEM) image of ZnO NPs and the average size of the ZnO particle was ~4 nm. The calculated size of ZnO NPs by UV-vis spectroscopy and XRD agreed well with the TEM observations. Fig. S1d shows the UV-vis spectra of fresh and stored ZnO NPs in chloroform solution. The synthesized ZnO NP solution showed good stability over 2 months.

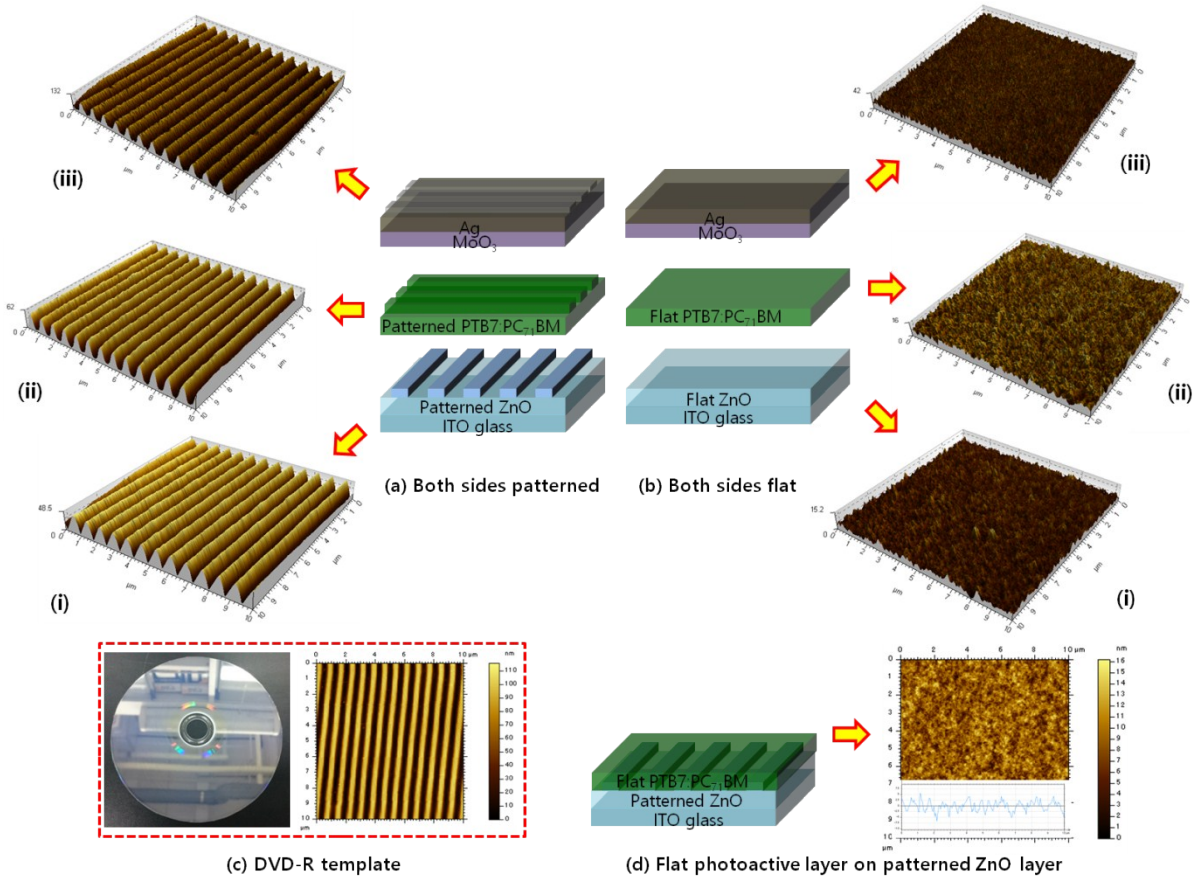

Fig. S2 AFM images of the surfaces in OPVs (a) with both sides patterned and (b) both sides flat. (a-i) p-ZnO layer, (a-ii) patterned PTB7:$PC_{71}BM$ layer spin-coated on the p-ZnO layer, (a-iii) MoO_3/Ag electrode deposited on the patterned PTB7:$PC_{71}BM$ layer, (b-i) f-ZnO layer, (b-ii) spin-coated PTB7:$PC_{71}BM$ layer on the f-ZnO layer, and (b-iii) MoO_3/Ag electrode deposited on the flat PTB7:$PC_{71}BM$ layer. (c) Photograph (left) and AFM image (right) of DVD-R master template. (d) AFM height image of the spin-coated PTB7:$PC_{71}BM$ layer on the p-ZnO layer, which showed no patterns on the surface.

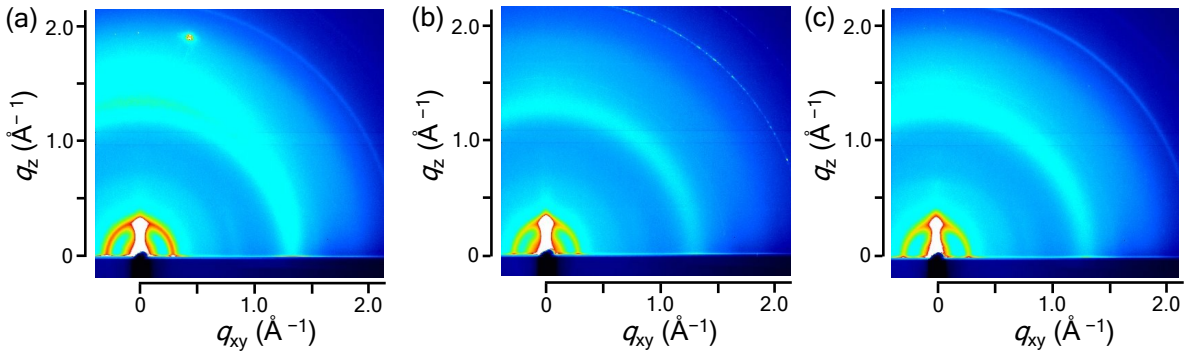

Fig. S3 2D GIWAXS patterns of the flat PTB7:$PC_{71}BM$ films deposited on (a) f-ZnO/ITO, (b) p-ZnO/ITO and (c) the surface patterned PTB7:$PC_{71}BM$ film on f-ZnO/ITO substrates.

2D GIWAXS patterns were measured at an incident angle of 0.12° using synchrotronradiation at beamline BL46XU of SPring-8 with the approval of the Japan Synchrotron Radiation Research Institute. The results in Fig. S3 show that although there may be difference of the total scattering intensity probably due to the difference in the interfacial or the surface roughness of the films, there was no large difference in term of the molecular orientation or the crystallinity of the polymer.

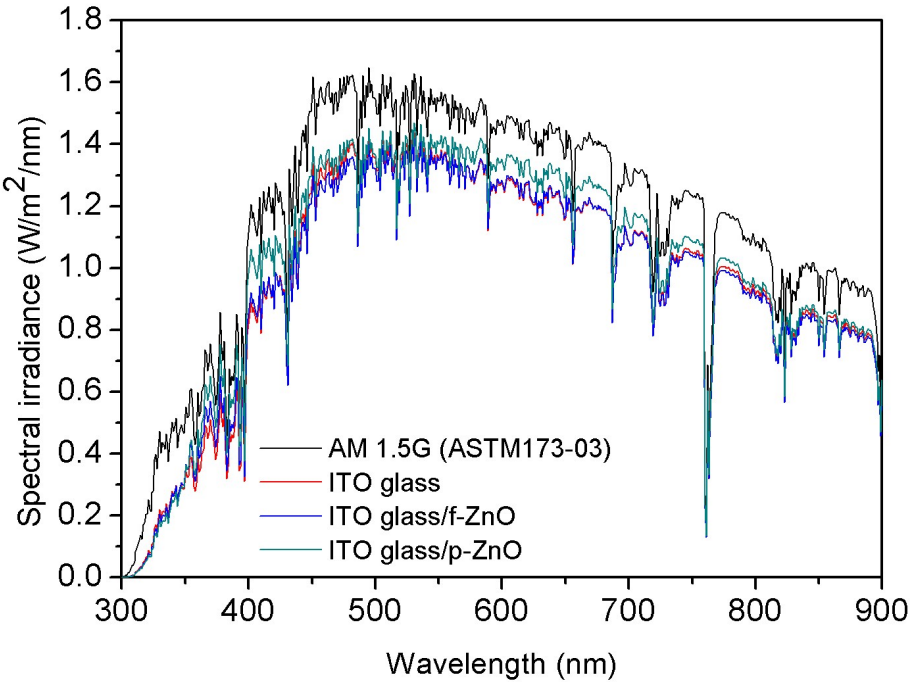

Fig. S4 Spectral distribution of the SWT for ITO/glass, f-ZnO/ITO glass, and p-ZnO/ITO glass calculated by using AM 1.5G spectral irradiance and measured transmittance spectra.

Calculation of solar weighted transmittance

To investigate the influence of the transmittance properties of p-ZnO layers on the performance of OPVs, the solar weighted transmittance (SWT), which is the ratio of the usable photons transmitted to the total usable photons, was calculated (Fig. S4).[2] The SWT can be evaluated by the optical transmittance spectra with the solar spectral irradiation (i.e., AM 1.5G solar spectral irradiance, ASTM G173-03 from NREL) integrated over a wavelength range of 300–900 nm.[3] The SWT is given by

$$SWT = \frac{\int_{300}^{900} I_s(\lambda)T(\lambda)d\lambda}{\int_{300}^{900} I_s(\lambda)d\lambda} \quad (1)$$

where $I_S(\lambda)$ is the spectral irradiance (i.e., AM 1.5G) and $T(\lambda)$ is the optical transmittance in Fig. 3a. The SWT value of the p-ZnO/ITO structure was 87.7%, which was higher than that for the f-ZnO/ITO structure (84.7%).

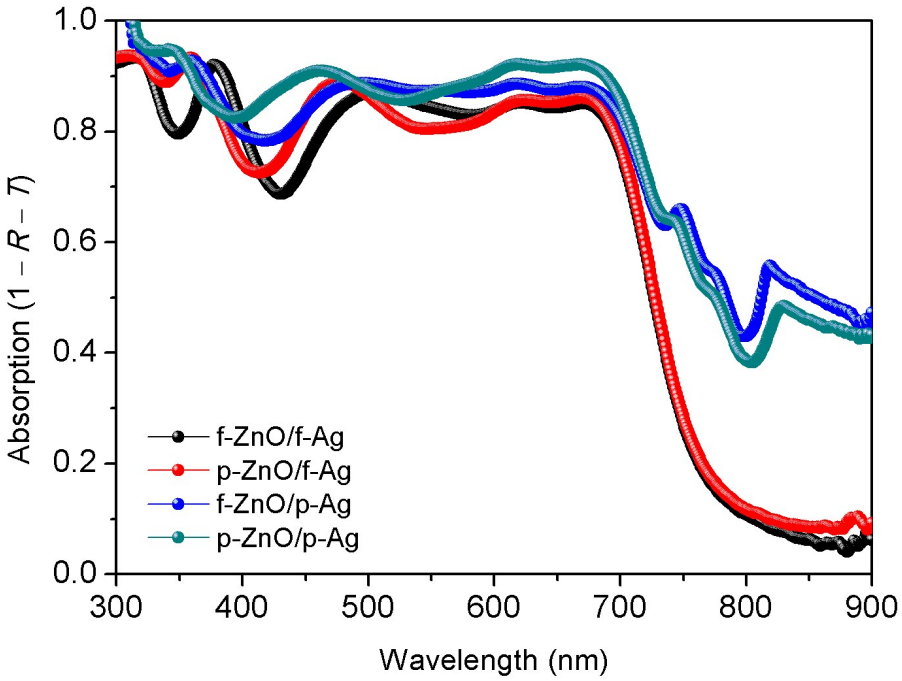

Fig. S5 Absorption ($1 - R - T$) properties of PTB7-based devices with structures of f-ZnO/f-Ag, p-ZnO/f-Ag, f-ZnO/p-Ag, and p-ZnO/p-Ag.

Calculation of solar weighted absorption

To quantify the change of the absorbed solar energy in the active layer, the solar weighted absorption (SWA) was also evaluated. The SWA is given by[4]

$$SWA = \frac{\int_{300}^{900} a(\lambda)S(\lambda)d\lambda}{\int_{300}^{900} S(\lambda)d\lambda} \quad (3)$$

where $a(\lambda)$ is the absorption spectrum in Fig. S5 and $S(\lambda)$ is the solar irradiance spectrum (i.e., AM 1.5G solar spectral irradiance, ASTM G173-03 from NREL). SWA values calculated for f-ZnO/f-Ag, p-ZnO/f-Ag, f-ZnO/p-Ag, and p-ZnO/p-Ag devices are 64.4%, 67.0%, 74.6%, and 78.1%, respectively.

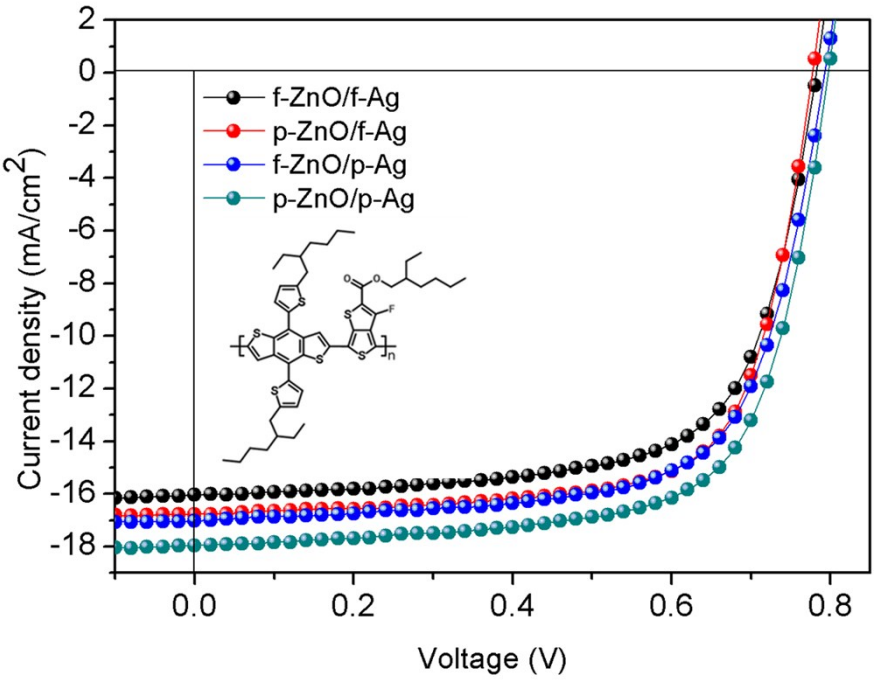

Fig. S6 *J-V* characteristics of OPVs based on PCE10:$PC_{71}BM$ with the structures of f-ZnO/f-Ag, p-ZnO/f-Ag, f-ZnO/p-Ag, and p-ZnO/p-Ag measured under AM 1.5 illumination at 100 mW cm^{-2}. The inset shows the chemical structure of PCE10.

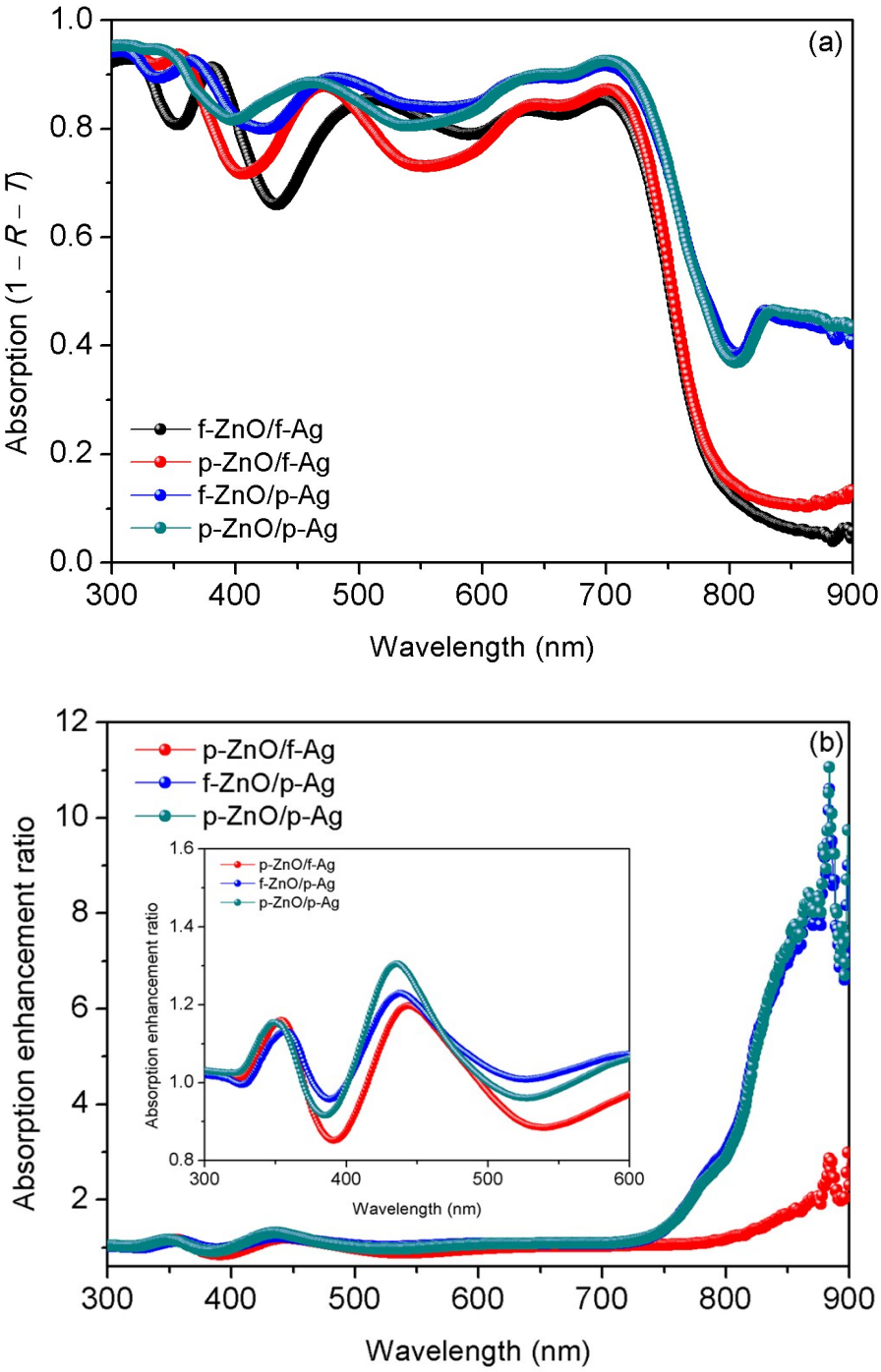

Fig. S7 (a) Absorption ($1 - R - T$) properties of the OPVs based on PCE10:$PC_{71}BM$ BHJ with structures of f-ZnO/f-Ag, p-ZnO/f-Ag, f-ZnO/p-Ag, and p-ZnO/p-Ag and (b) absorption enhancement ratios of the patterned devices relative to the reference (f-ZnO/f-Ag) with TM polarized light. The inset shows a magnified view in the range of 300 to 600 nm.

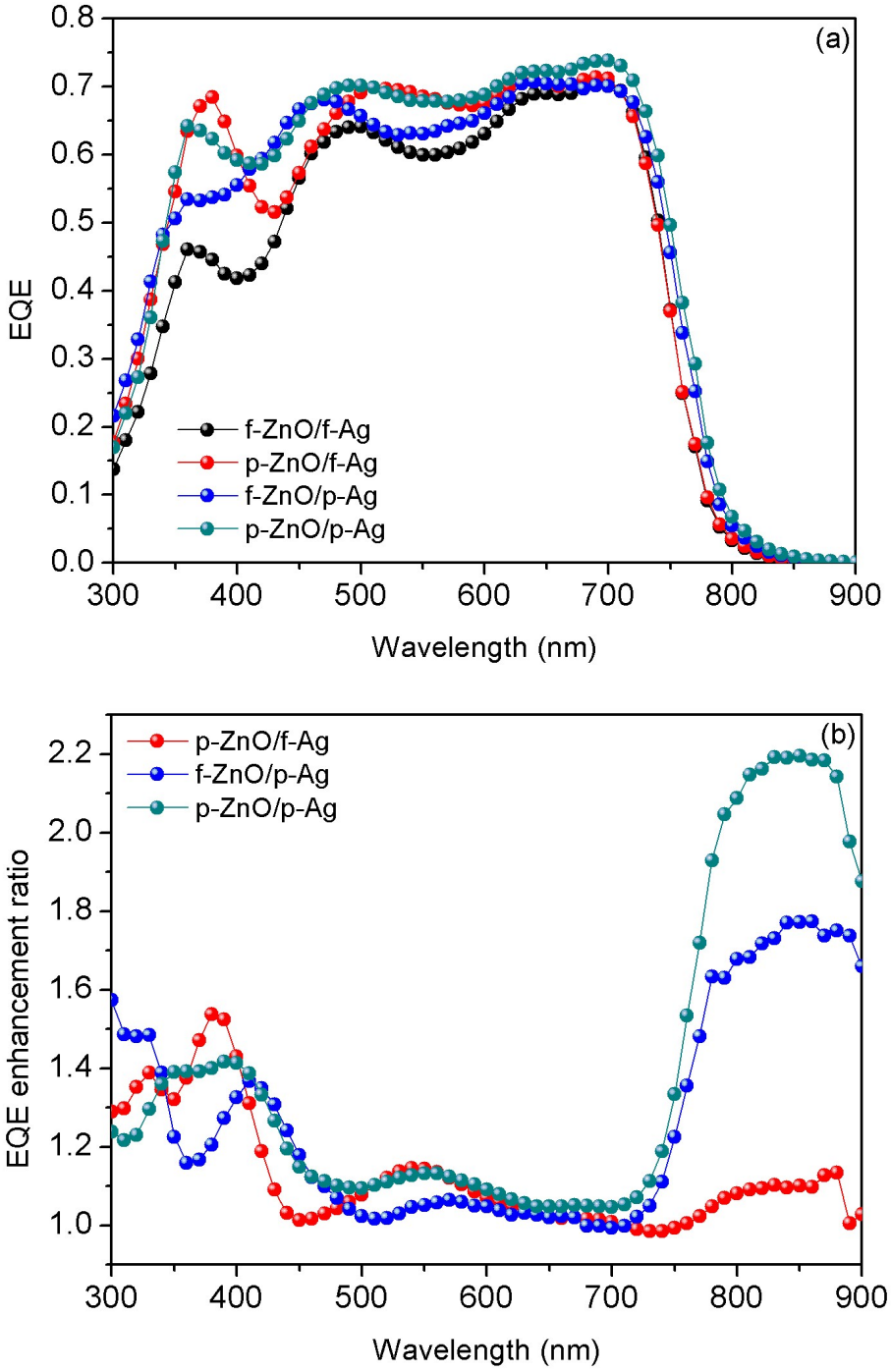

Fig. S8 (a) EQE spectra of the OPVs based on PCE10:$PC_{71}BM$ BHJ with structures of f-ZnO/f-Ag, p-ZnO/f-Ag, f-ZnO/p-Ag, and p-ZnO/p-Ag and (b) EQE enhancement ratios of the patterned devices relative to the reference device (f-ZnO/f-Ag).

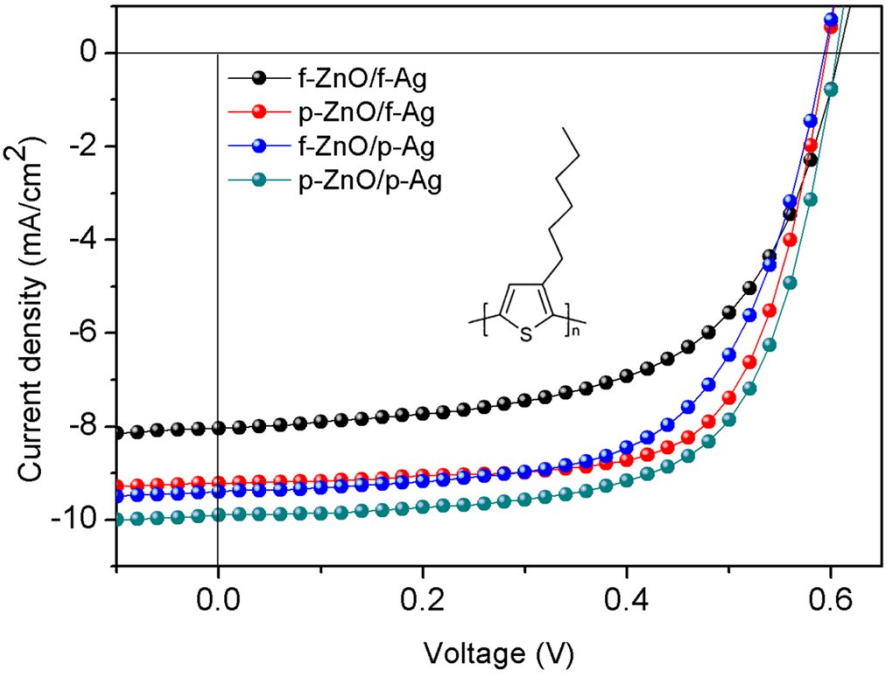

Fig. S9 *J-V* characteristics of OPVs based on P3HT:$PC_{61}BM$ with structures of f-ZnO/f-Ag, p-ZnO/f-Ag, f-ZnO/p-Ag, and p-ZnO/p-Ag measured under AM 1.5 illumination at 100 mW cm^{-2}. The inset shows the chemical structure of P3HT.

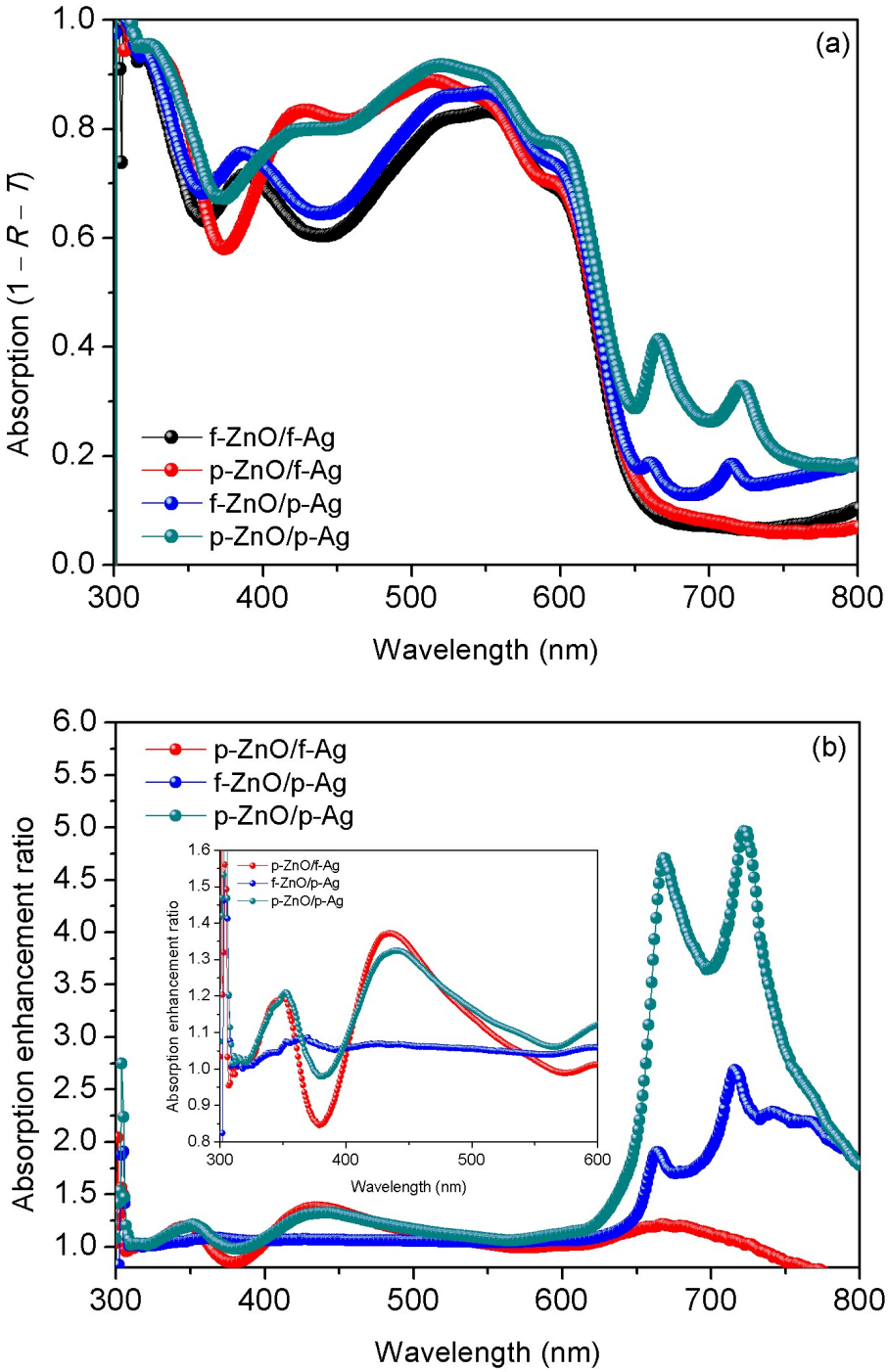

Fig. S10 (a) Absorption ($1 - R - T$) properties of the OPVs based on P3HT:$PC_{61}BM$ BHJ with the structures of f-ZnO/f-Ag, p-ZnO/f-Ag, f-ZnO/p-Ag, and p-ZnO/p-Ag and (b) absorption enhancement ratios of the patterned devices relative to the reference (f-ZnO/f-Ag) with TM polarized light. The inset shows a magnified view in the range of 300 to 600 nm.

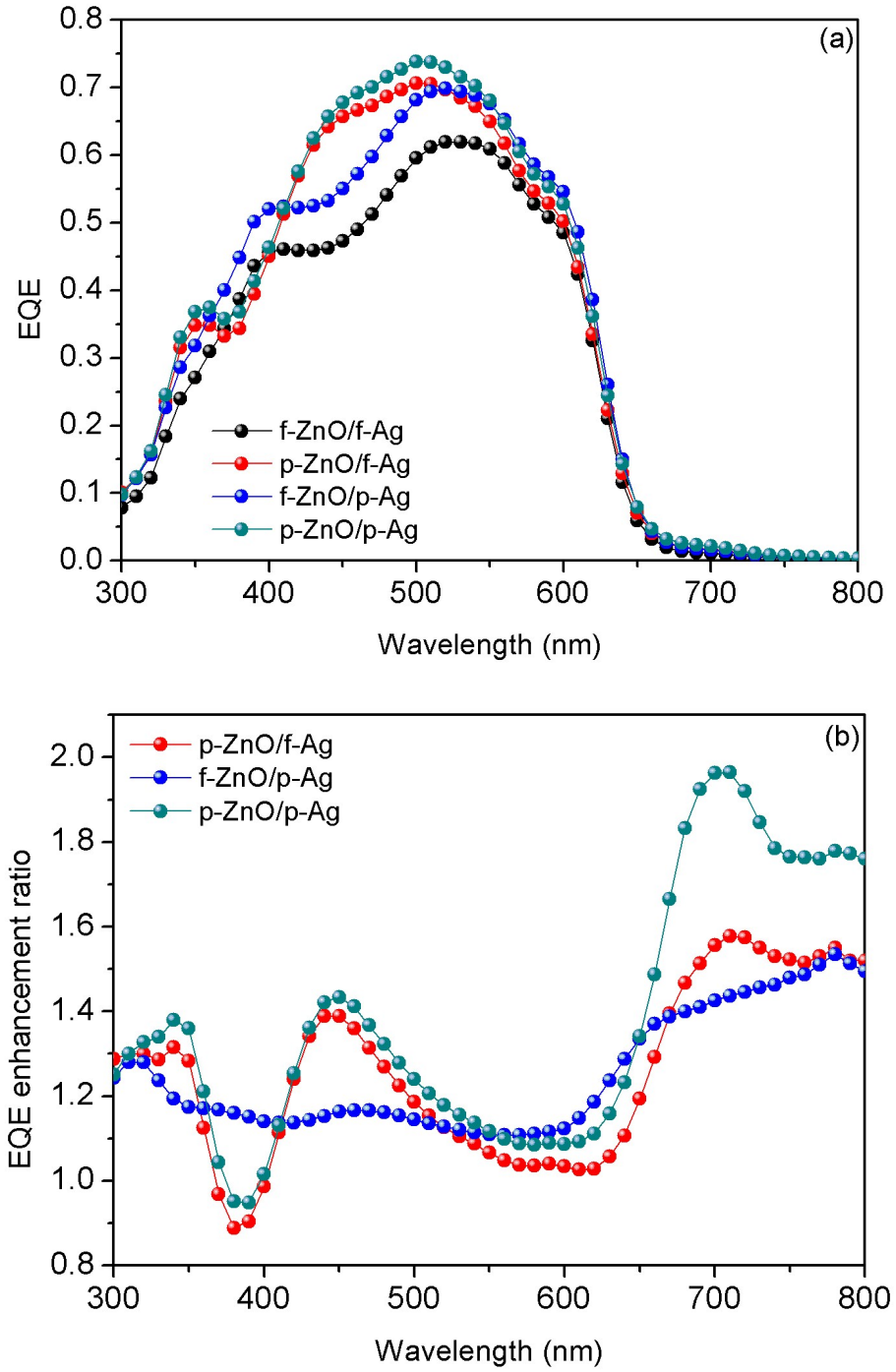

Fig. S11 (a) EQE spectra of the OPVs based on P3HT:$PC_{61}BM$ BHJ with structures of f-ZnO/f-Ag, p-ZnO/f-Ag, f-ZnO/p-Ag, and p-ZnO/p-Ag and (b) EQE enhancement ratios of the patterned devices relative to the reference device (f-ZnO/f-Ag).

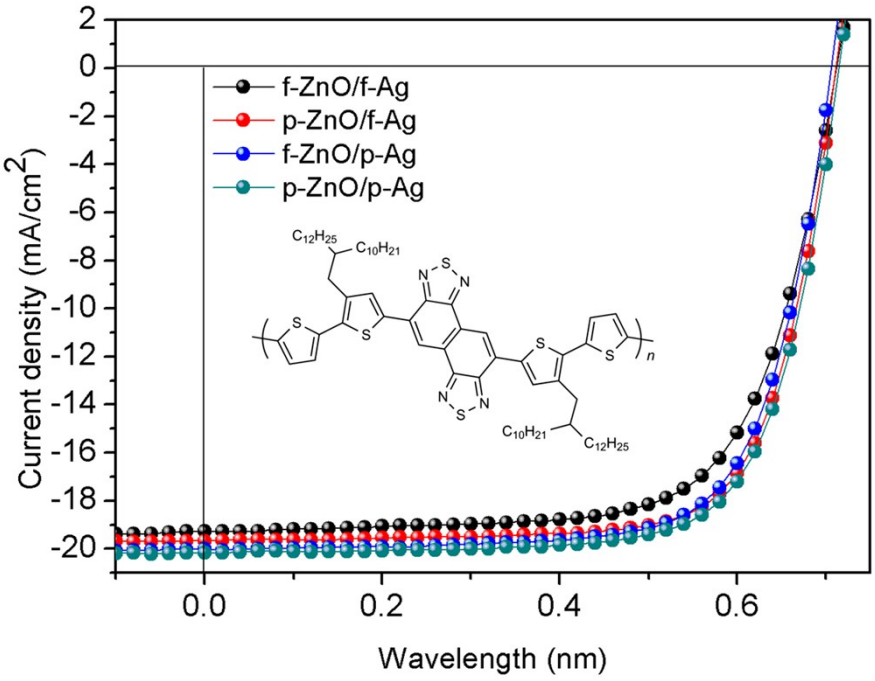

Fig. S12 *J-V* characteristics of OPVs based on PNTz4T:$PC_{71}BM$ with structures of f-ZnO/f-Ag, p-ZnO/f-Ag, f-ZnO/p-Ag, and p-ZnO/p-Ag measured under AM 1.5 illumination at 100 mW cm^{-2}. The inset shows the chemical structure of PNTz4T.

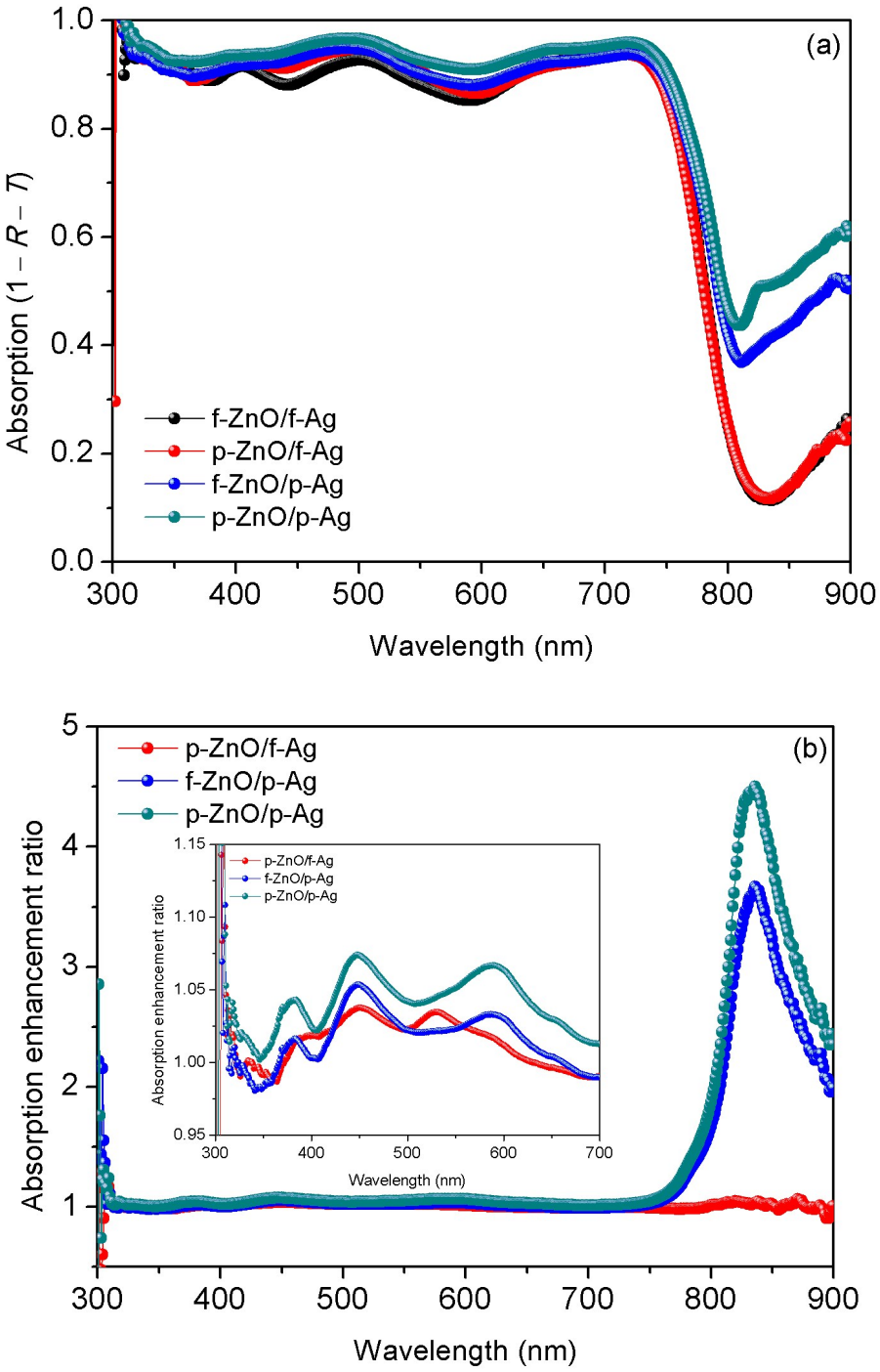

Fig. S13 (a) Absorption ($1 - R - T$) properties of the OPVs based on PNTz4T:$PC_{71}BM$ BHJ with structures of f-ZnO/f-Ag, p-ZnO/f-Ag, f-ZnO/p-Ag, and p-ZnO/p-Ag and (b) absorption enhancement ratios of the patterned devices relative to the reference (f-ZnO/f-Ag) with TM polarized light. The inset shows a magnified view of 300 to 600 nm.

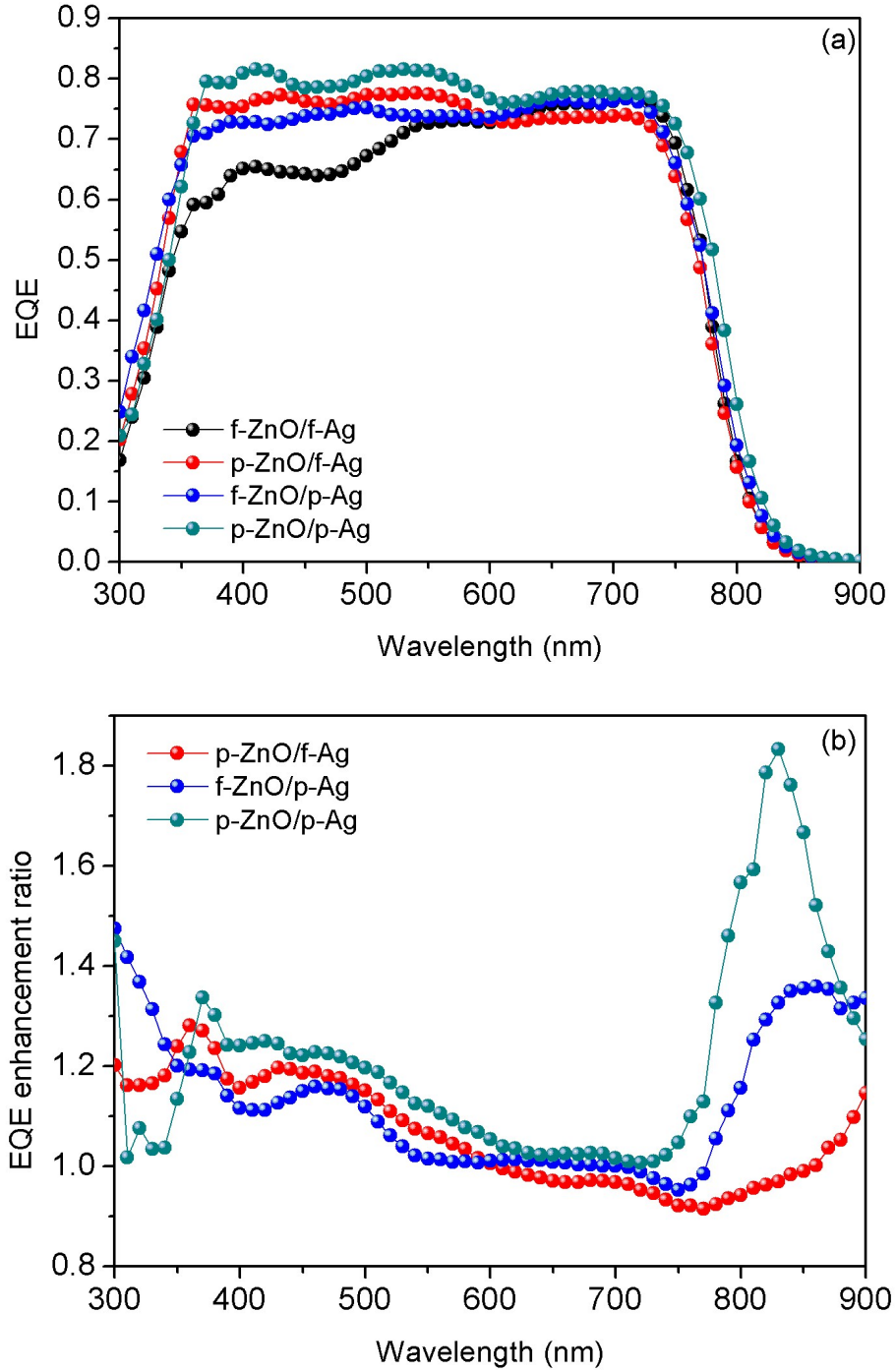

Fig. S14 (a) EQE spectra of the OPVs based on PNTz4T:$PC_{71}BM$ BHJ with structures of f-ZnO/f-Ag, p-ZnO/f-Ag, f-ZnO/p-Ag, and p-ZnO/p-Ag and (b) EQE enhancement ratios of the patterned devices relative to the reference (f-ZnO/f-Ag).

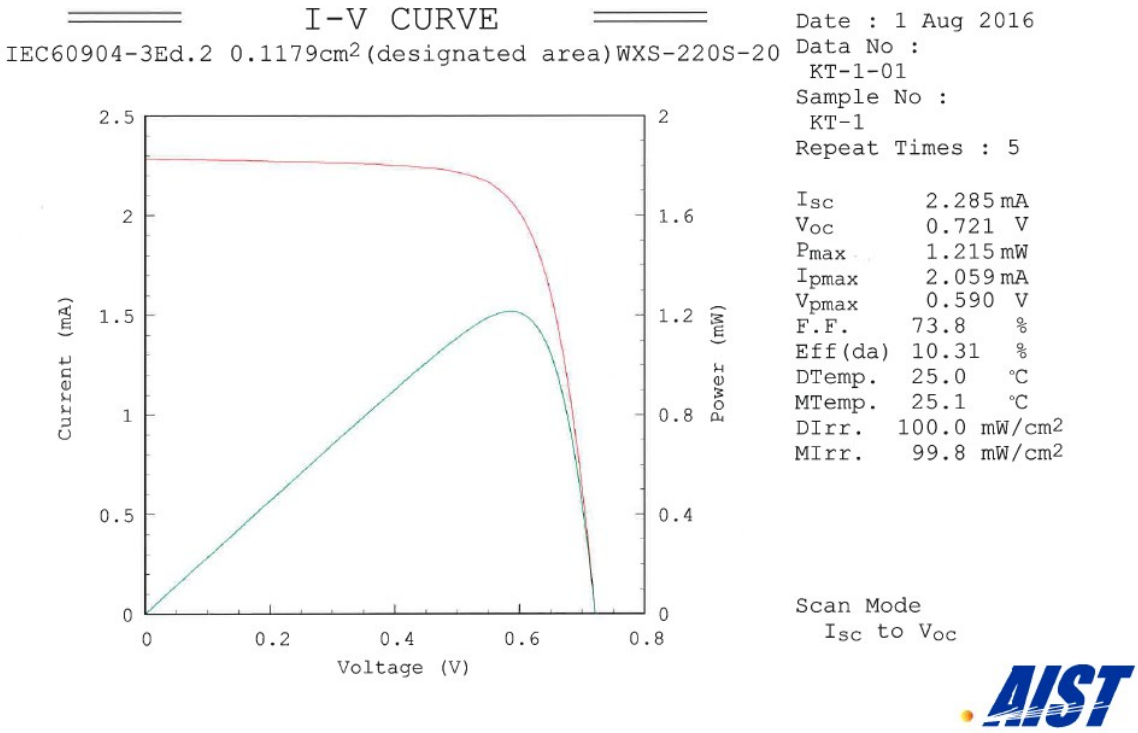

Fig. S15 PCE of 10.31% was certified for the PNTz4T:$PC_{71}BM$ device at the National Institute of Advanced Industrial Science and Technology (AIST).

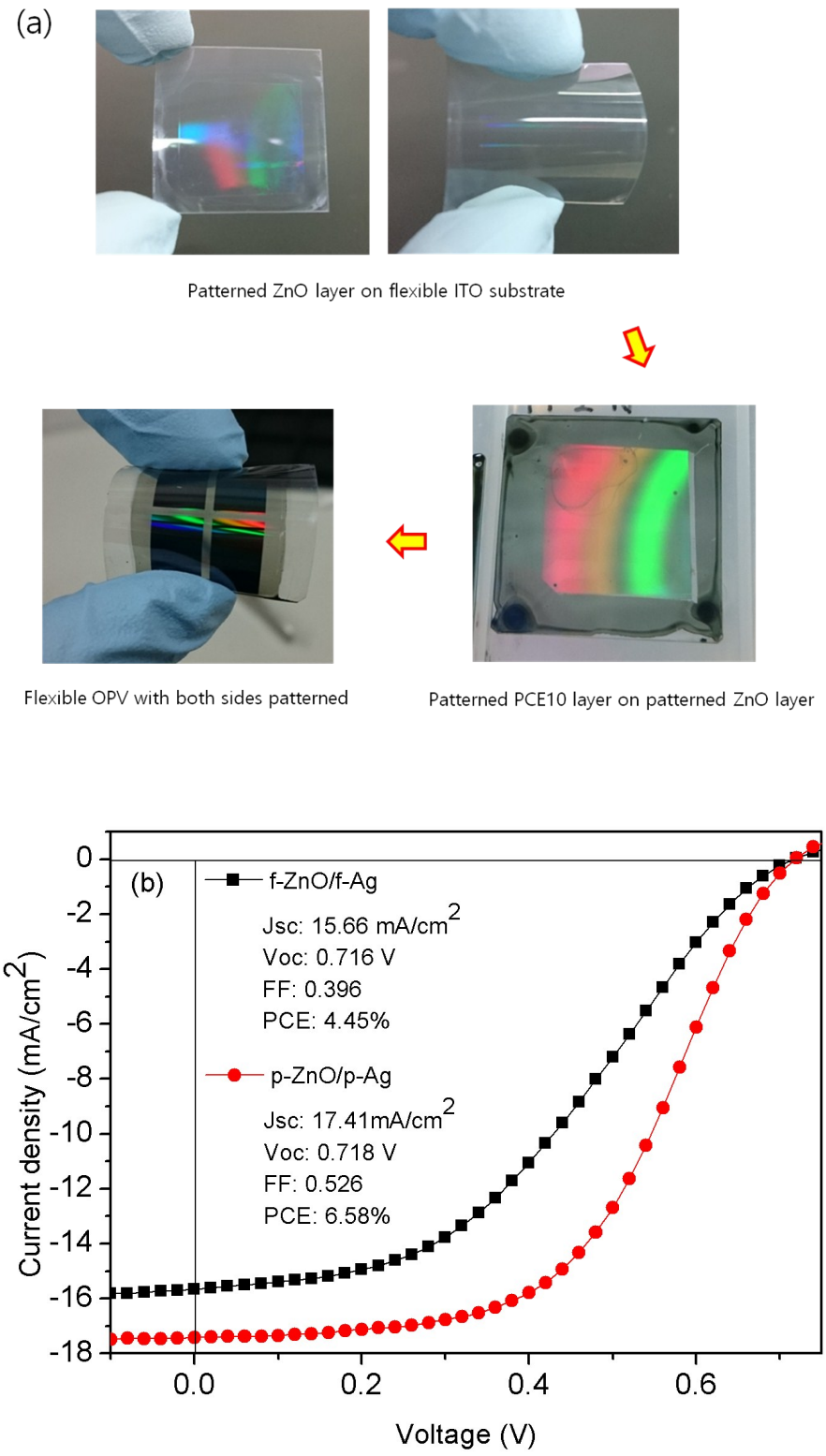

Fig. S16 (a) Schematic illustration of the fabrication of inverted flexible OPVs patterned on both sides by soft imprinting lithography by using a DVD template. (b) *J-V* characteristics of the flexible OPVs with interfaces that are either both flat or both patterned measured under AM 1.5 illumination at 100 mW cm^{-2}.

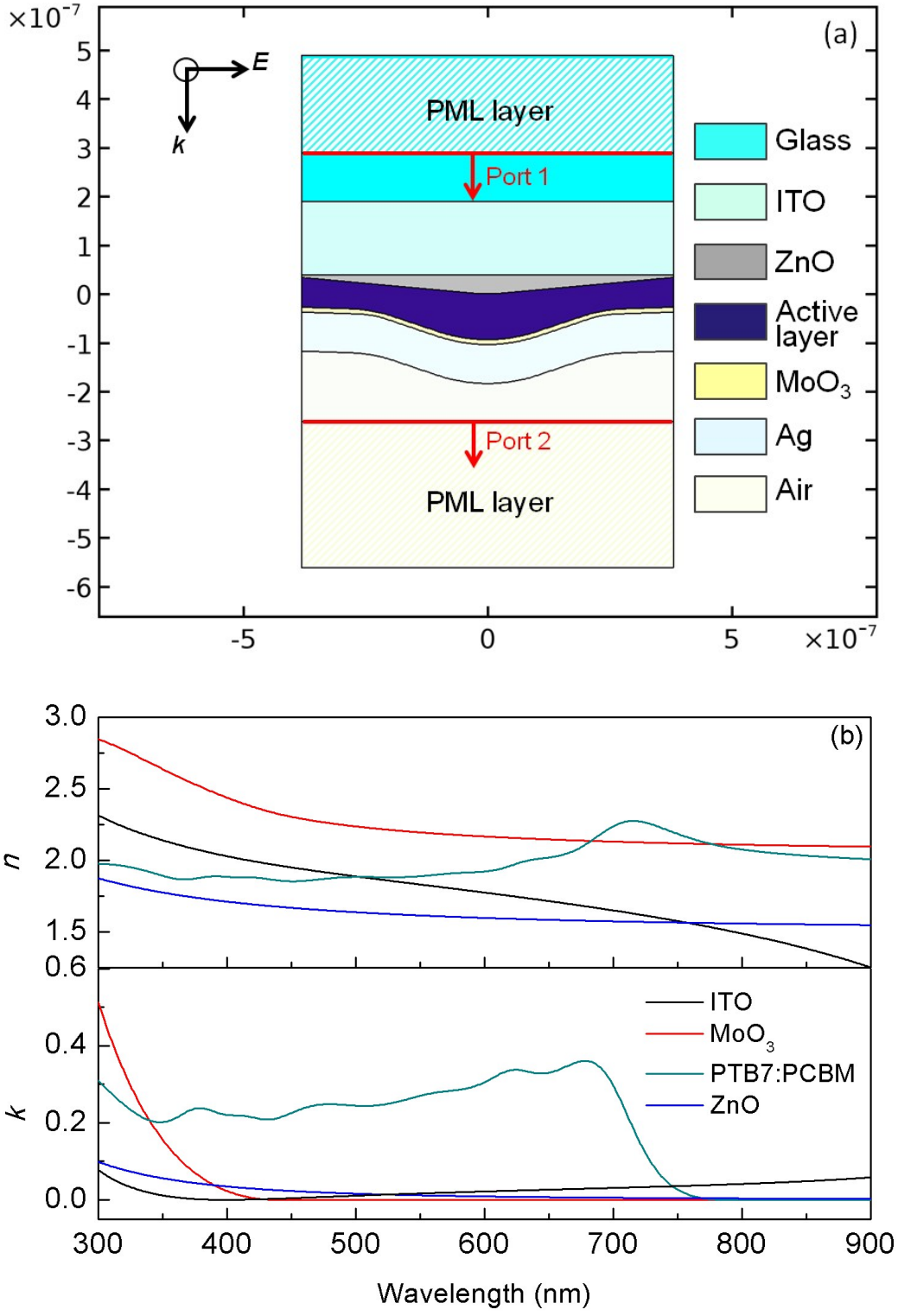

Fig. S17 (a) 2D-model of p-ZnO/p-Ag device for the numerical calculation by COMSOL and (b) refractive index (*n*) and extinction coefficient (*k*) of the materials used for the simulation. The optical constants were determined by spectral ellipsometry.

Table S1. Comparison of experimentally obtained J_{SC} from *J-V* characteristics and calculated J_{SC} from EQE spectra.

BHJ	Nanopattterns	J_{SC} [mA cm^{-2}]	J_{SC} (EQE) [mA cm^{-2}]	ΔJ_{SC} [%]	V_{OC} [V]	FF [%]	PCE [%]
PTB7: $PC_{71}BM$ (1:1.5)	f-ZnO /f-Ag	15.42 ± 0.04	14.80	4.1	0.72	67.7 ± 0.3	7.50 ± 0.06
	p-ZnO /f-Ag	15.96 ± 0.08	15.58	2.4	0.72	70.2 ± 0.9	8.16 ± 0.09
	f-ZnO /p-Ag	16.67 ± 0.15	15.73	5.9	0.72	68.1 ± 0.3	8.25 ± 0.1
	p-ZnO /p-Ag	17.23 ± 0.08	16.92	1.8	0.73	69.4 ± 0.2	8.72 ± 0.07
PCE10: $PC_{71}BM$ (1:1.5)	f-ZnO /f-Ag	16.07 ± 0.06	15.07	6.6	0.78	68.0 ± 0.3	8.54 ± 0.05
	p-ZnO /f-Ag	16.64 ± 0.08	16.16	2.9	0.78	70.7 ± 0.2	9.20 ± 0.04
	f-ZnO /p-Ag	17.27 ± 0.11	16.28	6.0	0.79	68.2 ± 0.1	9.28 ± 0.09
	p-ZnO /p-Ag	17.95 ± 0.07	17.11	4.9	0.79	69.2 ± 0.1	9.86 ± 0.02
P3HT: $PC_{61}BM$ (1:0.6)	f-ZnO /f-Ag	8.07 ± 0.05	7.94	1.6	0.60	58.4 ± 0.4	2.86 ± 0.04
	p-ZnO /f-Ag	9.20 ± 0.04	9.08	1.3	0.60	68.7 ± 0.1	3.79 ± 0.05
	f-ZnO /p-Ag	9.38 ± 0.05	9.10	3.0	0.58	62.8 ± 0.2	3.46 ± 0.04
	p-ZnO /p-Ag	9.88 ± 0.02	9.52	3.7	0.60	66.5 ± 0.3	3.96 ± 0.03
PNTz4T: $PC_{71}BM$ (1:2)	f-ZnO /f-Ag	19.06 ± 0.08	18.58	2.5	0.70	70.6 ± 0.3	9.45 ± 0.12
	p-ZnO /f-Ag	19.64 ± 0.09	19.28	1.8	0.71	73.1 ± 0.3	10.26 ± 0.03
	f-ZnO /p-Ag	20.01 ± 0.13	19.40	3.1	0.71	71.8 ± 0.4	10.19 ± 0.03
	p-ZnO /p-Ag	20.13 ± 0.10	20.12	0.1	0.71	72.5 ± 0.5	10.41 ± 0.07

References

1. E. A. Meulenkamp, *J. Phys. Chem. B*. 1998, **102**, 5566.

2. J. W. Leem, S. Kim, S. H. Lee, J. A. Rogers, E. Kim, J. S. Yu, *Adv. Energy Mater*. 2014, **4**, 1301315.

3. H. Cui, S. Pillai, P. Campbell, M. A. Green, *Sol. Energy Mater. Sol. Cells*. 2013, **109**, 233.

4. C. Min, J. Li, G. Veronis, J. Y. Lee, S. Fan, P. Peumans, *Appl. Phys. Lett*. 2010, **96**, 133302.